

显微集成术中光学相干断层血流造影术

张子艺¹, 俞晨阳¹, 乔依琳³, 沈丽君³, 程丹³, 李鹏^{1, 2*}

¹浙江大学光电科学与工程学院, 浙江 杭州 310027;

²浙江大学嘉兴研究院智能光电创新中心, 浙江 嘉兴 324000;

³温州医科大学附属眼视光医院杭州院区眼底病专科, 浙江 杭州 310020

摘要 提出一种集成手术显微镜的术中光学相干血流造影系统(iOCTA)来实现术中眼底视网膜血流灌注的动态监测。通过光学相干断层扫描血管造影(OCTA)系统的光路与商用手术显微镜的助手镜的成像光路耦合,实现显微镜-OCTA的系统集成,这种简捷的耦合方式便于现有手术显微镜的功能升级。采用基于逆信噪比和去相关的光学相干血流运动造影(ID-OCTA)算法,实现高信噪比的眼底微血管成像。利用该系统实现了活体兔眼的术中眼底血流灌注成像,揭示了血流灌注随眼内压的时空动态演变过程,发现急性高眼内压(60 mmHg; 1 mmHg = 133.32 Pa)将导致血流灌注密度值在短时间内降低至基线值的 20% 以下。所研制的 iOCTA 系统有望实现眼科手术中眼底血流灌注的实时监测,有助于外科医生客观评价手术过程和预测术后效果。

关键词 医用光学; 生物医学成像; 光学相干层析成像; 光学相干血流造影; 术中成像

中图分类号 TN247

文献标志码 A

DOI: 10.3788/CJL202249.1507301

1 引言

眼科手术中,眼组织中的血流灌注信息是外科医生判定患者当下眼组织生理功能、病理状态和术后并发症的重要依据。例如,在白内障超声乳化手术或玻璃体切除术等眼科手术中,患者的眼内一般会产急性眼内压波动,当眼内压的变化超出眼底血管的代偿能力时,可能导致血管受损,增加术后并发症的发生率^[1-3]。然而,目前在术中常用的辅助工具为手术显微镜,其成像结果中仅包含有限的表层血管信息,且毛细血管和视网膜组织之间的对比度较低,难以观察和量化血管内的血流灌注状态。

荧光血管造影技术是评估视网膜和脉络膜血流特征的传统方法,具有分辨单根血管的能力。然而,对于血流成像效果,传统的荧光血管造影在成像深度、视场及深度方向的分辨能力受限;对于受试者,荧光血管造影需要注射荧光标记物,具有侵入性,可能引发恶心或严重的过敏等一系列副作用,多次染色导致的染料残留还可能造成血管细节混淆^[4-5]。因此,荧光血管造影并非最佳的术中眼底血流监测方法,需要一种有效的血流灌注成像手段来实现非侵入、无需染色、毛细血管水平的术中三维血流监测。

光学相干断层扫描血管造影(OCTA)技术作为光

学相干断层成像(OCT)技术的功能扩展,将血红细胞与周围组织的相对运动作为内源性血流标记特征,不需要外源性荧光标记物,可提供活体、无创、无接触、无标记和毛细血管水平的三维血流灌注成像结果^[6-12]。高速 OCT 系统和高效 OCTA 算法的发展进一步促进了 OCTA 的临床实践,提供了有价值的医学生理信息^[13-20]。

得益于 OCT 的深度分辨能力和 OCTA 的血流造影能力,国际上多个研究小组开展了集成 OCT 和 OCTA 的手术显微镜研究。术中 OCT(iOCT)可以实时获得手术中眼组织或手术器械的三维空间结构的动态变化,每个 A-line 的采集速度达到 100 kHz^[21-27]。多项临床评估结果表明,通过 iOCT 观察角膜移植术中的剩余基质薄层或视网膜剥膜术中的残留组织,有助于防治术后并发症^[28-33]。通过进一步集成 OCTA 技术,术中 OCTA(iOCTA)可以在手术中实现三维血流成像^[34-35]。Chen 等^[34]开展了儿童视网膜病变区域的 iOCTA 研究,通过血流造影成像实现手术效果评价;但是,在该研究中显微镜和 OCTA 之间采用了复杂的耦合方式,需要拆装原显微镜,并改变原显微镜符合人体工程学的轴向尺寸,难以实现现有商用手术显微镜的改造升级。Zhang 等^[35]开发了一种 iOCTA 系统,初步实现了小鼠脑部的血流灌注成像,进一步优化

收稿日期: 2021-12-01; 修回日期: 2022-01-18; 录用日期: 2022-01-26

基金项目: 国家自然科学基金(62075189)、国家自然科学基金青年科学基金项目(81900910)、浙江省自然科学基金(LR19F050002)、浙江省自然科学基金探索项目(LQ19H120003)、之江实验室项目(2018EB0ZX01)

通信作者: * peng_li@zju.edu.cn

耦合光路和聚焦光路后,可实现眼底视网膜的高分辨率成像。上述 iOCTA 技术均是基于扫频光源实现的,但是扫频光源的相位不稳定,通常使用强度信号来提取血流信息,造成血流对比度受限。

本文发展了一种可实现术中结构和血流造影成像的 iOCTA 系统。该系统在商用手术显微镜的基础上,设计了简捷可靠的光机结构,在保持手术显微镜在轴向上的人体工程学设计的同时,实现了 OCT 模块与手术显微镜模块的同步聚焦;引入基于逆信噪比和去相关的光学相干血流运动造影(ID-OCTA)算法,并采用相位较稳定的谱域 OCT 系统,实现了高分辨的三维血流灌注成像。为了验证该系统在术中血流成像的可行性,本文设计了眼科模拟手术并在术中全程监测眼底血流灌注状态。在术中各关键阶段,该 iOCTA 系统实时获取了高分辨的眼底血流灌注结果,并通过定量的纵向分析揭示了血流灌注随眼内压的时空动态演变过程,有助于外科医生在术中即时掌握患者眼底血流状态并做出正确的决策。

2 基本原理

2.1 系统搭建

本实验涉及的 iOCTA 系统的整体光路结构如图 1 所示,主要分为 OCT 模块和手术显微镜模块。OCT 模块基于典型的谱域 OCT 结构,其核心部件包括光源、参考臂、样品臂和探测器。光源采用中心波长

为 850 nm、半峰全宽为 100 nm 的超辐射发光二极管(SLD)宽带光源,其输出的 OCT 成像光束经过光纤耦合器后分别进入参考臂和样品臂,参考臂光束入射至反射镜镜面后形成参考光返回,样品臂光束入射至样本表面后携带样本信息返回,二者在光纤耦合器相遇后形成干涉信号,由线扫速率为 120 kHz 的光谱仪线阵相机 camera 1 接收,可实现空气中轴向分辨率为 $2.3 \mu\text{m}$ 、深度方向量程为 2.6 mm、信噪比为 102 dB 的 OCT 成像。在样品臂中,OCT 成像光束经 X-Y 型振镜扫描和透镜组扩束后,通过手术显微镜 OPMI Lumera 300 (Carl Zeiss, Germany) 的第二辅助接口与手术显微镜的成像光束耦合;OCT 模块与手术显微镜模块共用焦距为 200 mm 的显微物镜,可实现理论横向分辨率为 $13.4 \mu\text{m}$ 的 OCT 三维成像。该耦合方式所设计的耦合器件与手术显微镜侧面的助手镜接口结构相匹配,在保持手术显微镜轴向的人体工程学设计的同时,实现了显微镜-OCT 光路集成。手术显微镜模块采用术中眼底观察系统(Oculus, Germany)实现眼底成像,采用面阵相机 camera 2 获取显微镜的实时成像结果,采用可调位移台承载手术样本。在手术过程中,外科医生能够通过显示屏用户界面的相机 camera 2 实时画面或显微目镜观察手术样本的组织表面,通过用户界面的实时 OCT 或 OCTA 画面观察手术样本的组织深层信息,实现对眼科手术的监测和导航。

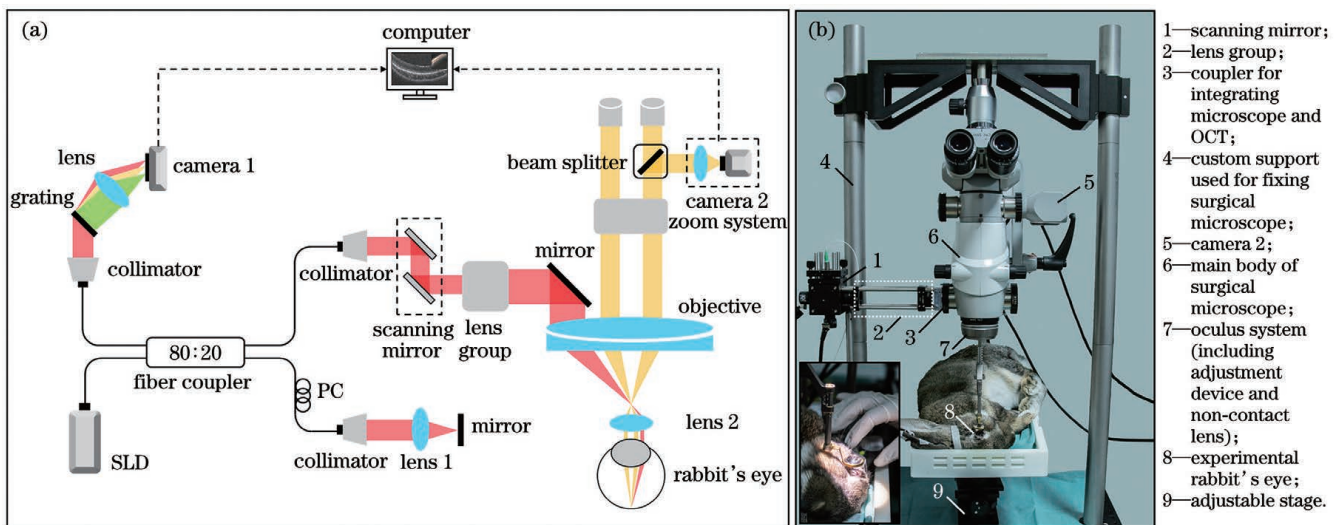


图 1 集成手术显微镜的 iOCTA 系统。(a)系统光路结构示意图(lens 2 为眼底观察系统的非接触镜,常见的光焦度为 120 D 或 200 D);(b)样品臂和实验兔子

Fig. 1 iOCTA system based on a standard surgical microscope. (a) Schematic of system lightpath (lens 2 is a non-contact lens, common focal powers are 120 D or 200 D); (b) sample arm and experimental rabbit

在本实验搭建的 iOCTA 系统中,控制振镜扫描范围以获取三维 OCT 体数据(Z-X-Y),该扫描范围对应的兔眼视网膜组织上的成像范围约为 $2.6 \text{ mm} \times 3 \text{ mm} \times 3 \text{ mm}$ 。其中,每个 B-frame 在快扫描(X)方向包含 400 A-line,在每个位置连续获取 3 个 B-frame 用于血流成像的去相关值计算,在慢扫描(Y)方向共

采样 400 个位置,总采集时间约为 4.8 s。

2.2 动物准备

为了验证 iOCTA 系统生成术中血流成像结果的可行性,实施了眼科手术模拟实验,并在实验中全程使用该 iOCTA 系统进行实时监测。本次眼科模拟手术的实验对象为 3 只体重为 2.5~3.0 kg 的雄性灰兔(生

产许可证号:SCXK(京)2014-0004),所有动物实验程序均符合视觉和眼科研究协会(ARVO)关于在眼科和视觉研究中使用动物的声明,并经浙江大学动物护理和使用委员会批准。将动物置于通风笼中饲养,饲养环境为12 h光周期(12 h光照,12 h黑暗),温度为20~26℃,相对湿度为40%~70%;标准饲料喂养,饮水量不限制;每周更换垫料2次,适应性饲养1周。

本手术模拟实验通过肌注盐酸塞拉嗪(0.1 mL/kg)和耳缘静脉注射戊巴比妥钠(42 mg/kg)麻醉灰兔后,以合适体位将其固定于iOCTA系统的样本台上,并为其佩戴开睑器以避免其眼睑闭合影响手术操作。术前滴加复方托吡卡胺滴眼液用于兔眼散瞳,滴加盐酸丙美卡因滴眼液辅助麻醉。术前和术后均滴加左氧氟沙星滴眼液和普拉洛芬滴眼液用于兔眼消毒。使用2%碘伏及75%乙醇溶液浸泡消毒各手术器械。

本手术模拟实验通过人为改变兔眼眼内压来模拟白内障超声乳化手术或玻璃体切除术中的眼内压波动。根据实际眼科手术的常用操作流程,制定该手术模拟实验的主要步骤如下:1)使用23 G巩膜穿刺刀于兔眼角巩膜缘向外2 mm处实施穿刺,制造手术通道;2)通过穿刺口连接灌注管及平衡盐溶液瓶,并缓慢升高溶液瓶,使兔眼眼内压在1 min内升高至目标值60 mmHg(1 mmHg = 133.32 Pa);3)灌注持续10 min后降低平衡溶液瓶,使兔眼眼内压在1 min内恢复为初始眼内压;4)保持兔眼眼内压稳定1 h。选择灰兔的右眼作为实验眼,实施上述手术模拟实验步骤;选择该灰兔的左眼作为对照眼,其实验操作与右眼在施加灌注前完全一致,但后续将维持左眼稳定的眼内压,与右眼波动的眼内压形成对照。在实验过程中,全程使用iOCTA系统实时采集兔眼视网膜血流灌注状态的图像。本次模拟实验对3只雄性灰兔完整实施了上述实验操作,3次实验均由同一实验员完成。

2.3 血流成像及量化

在每组手术模拟实验的各个阶段,分别选取若干有代表性的时间点进行术中血流成像。考虑到血流监测的准确性,本实验在眼内压变化剧烈的时间段设置了较高的采集密度,采集次数及采集时间点具体包括:第一阶段2次(未实施穿刺时1次、实施穿刺后1次)、第二阶段4次(施加灌注中的第1,3,5,10 min)、第三阶段11次(去除灌注后的第1,3,5,10,15,20,25,30,40,50,60 min)。

为了准确区分动态血流区域和静态周围组织,采用基于逆信噪比和去相关的光学相干血流运动造影(ID-OCTA)算法,在ID空间沿静态信号分布的 3σ 边界处设置分类线,剔除静态周围组织,保留动态血流区域,实现了活体、无创、无接触、无标记、毛细血管水平的三维血流灌注成像^[36-40]。感兴趣的三维组织区域的动态信号将在深度(Z)方向上投影成二维图像(en-face图像),以直观地展示血管系统和血流灌注情况。

在获取各时间点的兔眼三维血流成像结果后,进行基于兔眼视网膜血流 en-face 图像的量化分析。利用血管本身的特有结构作为区域选择的标志物,选取的各成像结果均包含血流区域,使每个采集时间点对应的成像结果中所选的血流区域一致。将这些血流区域以相同的阈值进行二值化,其中白色像素为血流像素数目 S_{OCTA} 。设所选区域的像素点总数为 S_n ,则第*i*个血流成像结果的血流密度计算公式为

$$S(i) = S_{\text{OCTA}}(i) / S_n(i). \quad (1)$$

为了更显著地描绘兔眼视网膜术中血流灌注随眼压的波动程度,以仅实施穿刺对应的血流密度($i=2$)值作为基线值,对各血流密度值进行归一化处理得到相对血流密度,第*i*个相对血流密度 $R_{\text{VD}}(i)$ 的计算公式^[41]为

$$R_{\text{VD}}(i) = \frac{S(i) - S(2)}{S(2)}. \quad (2)$$

在计算各兔眼视网膜的相对血流密度结果后,对3次实验的数据集进行均值及方差计算,得到手术模拟实验中兔眼视网膜术中血流灌注变化的综合结果。

3 iOCTA 图像及量化结果

3.1 兔眼视网膜在毛细血管水平的三维血流灌注成像结果

所提iOCTA系统的三维血流灌注结果可成像至毛细血管水平。如图2(a)所示,在OCT断层结构图像中,可以观察到兔眼的视网膜、脉络膜等结构。利用ID-OCTA算法对同一位置的3帧OCT结构断层图像进行OCT散射信号动态分析,生成去除周围组织的静态信号、保留血流灌注的动态信号的分类线[图2(c)],进而生成该位置的OCTA断层血流图^[36][图2(b)]。为了方便观察血流情况,整合400个位置的兔眼眼底OCTA断层血流图像,并选取视网膜层的血流灌注在深度(Z)方向上进行最大值投影,得到兔眼视网膜血流灌注的en-face图像[图2(d)],从该图像可以清晰地观察到兔眼视网膜的大血管和各毛细血管分支。视网膜OCTA的en-face图像和利用手术显微镜相机拍摄的视网膜血管图像[图2(e)]有一致的视网膜血管整体形态和分布,并且视网膜OCTA图像在毛细血管水平上有更丰富且对比度更高的成像细节。

3.2 iOCTA系统在模拟手术中的实时监测结果

与手术显微镜结合的OCTA技术是监测术中血流灌注变化的理想工具,可获取毛细血管水平的三维血流灌注图像并进行血流密度等定量分析。图3展示了在一次模拟手术全过程中一部分代表性时间点的兔眼视网膜血流灌注成像结果,其中阶段I为施加灌注前,阶段II的术中眼内压急性增加并保持在60 mmHg,阶段III的术中眼内压急性降低并保持初始的正常值。可以观察到在术中眼内压急性增加的阶段,视网膜血流灌注在1 min内整体显著减少,具体表

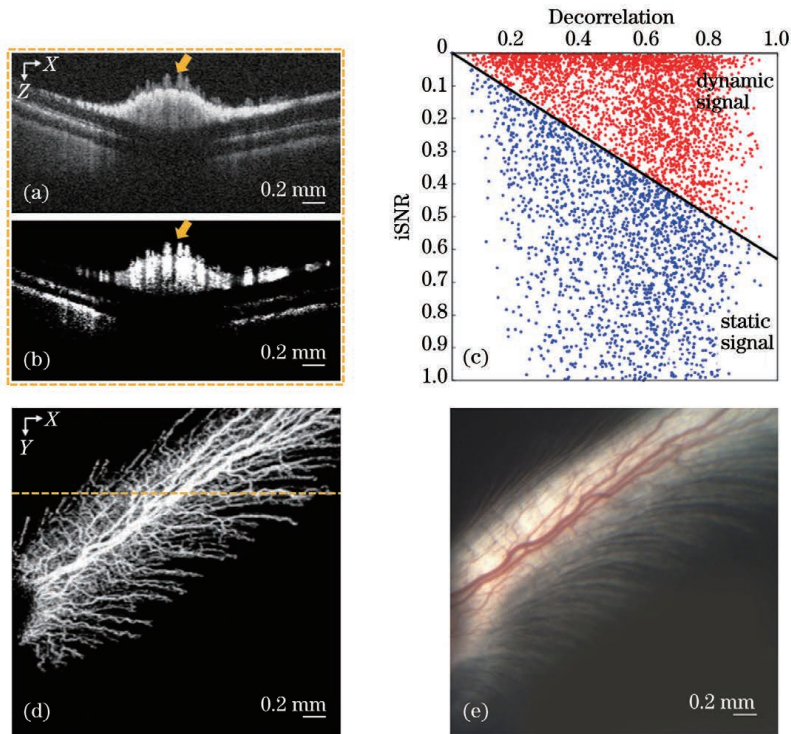


图 2 活体兔眼视网膜的血流灌注成像结果。(a)OCT 二维断层结构图,箭头标注的是视网膜大血管结构;(b)OCTA 二维断层血流图,箭头标注的是视网膜大血管血流,与(a)的大血管结构对应;(c)OCT 信号散点示意图,其中黑色斜线为 ID-OCTA 算法生成的分类线;(d)视网膜血流区域 OCTA 的 en-face 图像,黄色虚线为(a)、(b)对应的位置;(e)利用手术显微镜相机拍摄的图像

Fig. 2 Results of blood perfusion mapping in rabbit's retina. (a) OCT structural cross-section, and the arrow marks retinal big vessels; (b) OCTA cross-sectional angiogram, and the arrow marks big vessels which correspond to (a); (c) distribution of OCT signals, where black line is the classification line generated by ID-OCTA algorithm; (d) en-face image of OCTA, and dashed line is the position of (a) and (b); (e) image captured by camera of iOCTA system

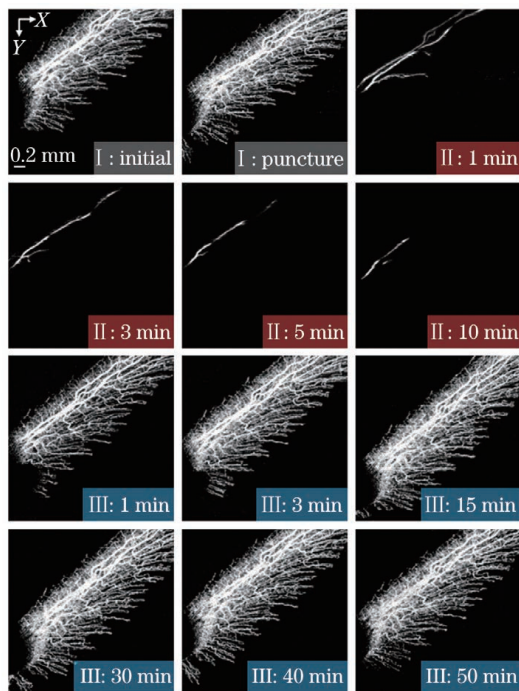


图 3 术中兔眼视网膜血流灌注随眼内压的动态变化

Fig. 3 Dynamic changes of intraoperative blood perfusion in rabbit's retina during acute intraocular pressure (IOP) fluctuations

现为大血管直径略有减小,毛细血管灌注几乎消失;在维持 60 mmHg 术中眼内压的 10 min 内,视网膜血流灌注有逐渐减少的趋势;在术中眼内压急性降低至初始值时,视网膜血流灌注在 3 min 内迅速恢复,具体表现为大血管管径整体恢复至施加灌注前的初始状态,毛细血管恢复血流灌注,并随着恢复时间的推移,血流的充盈程度略超过初始值。

为了更准确地分析术中血流灌注变化,对术中兔眼视网膜血流灌注进行了定量纵向分析。图 4 展示了三次模拟手术全过程中各阶段代表性时间点的兔眼视网膜血流灌注的相对血流密度分析结果,将仅实施穿刺对应的血流密度值作为此相对血流密度变化曲线的基线值,实线为实验眼的相对血流密度,实施了完整的模拟手术;虚线为对照眼的相对血流密度,在穿刺前和仅实施穿刺后 20 min 内进行术中成像,和实验眼的血流密度变化最剧烈的阶段形成鲜明对比。从血流密度变化曲线可以观察到:在术中眼内压急性增加时,视网膜相对血流密度均值在 1 min 内显著下降至基线值的 20% 以下;在维持 60 mmHg 术中眼内压的 10 min 内,视网膜相对血流密度均值以平稳的趋势缓慢下降;在术中眼内压急性降低至初始值时,视网膜相对血流密度均值在 3 min 内迅速上升,并随着恢复时间的推

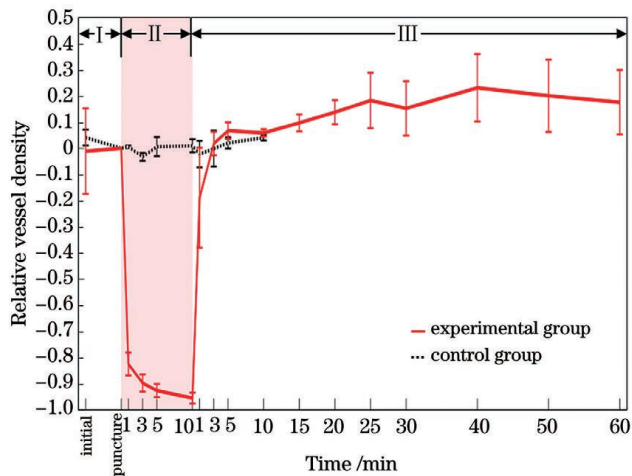


图4 术中兔眼视网膜相对血流密度随眼内压动态变化的量化结果(三只兔眼的平均结果)

Fig. 4 Quantitative results of dynamic changes of relative vessel density in rabbit's retina during acute IOP fluctuations (average result of 3 rabbits' eyes)

移,以平稳的趋势缓慢上升至略超过初始值。相对血流密度变化趋势在各代表性时间点与兔眼视网膜血流灌注的 en-face 图像一一对应。

4 分析与讨论

本实验提出一种可实现高分辨术中结构和血流造影成像的 iOCTA 系统。目前,对于术中应用的研究主要集中在结构成像^[23,28,31]。实际上,术中血流灌注的实时成像可为多种眼科手术提供监测和指导。例如:在白内障超声乳化手术或玻璃体切除术等存在眼内压急剧波动的眼科手术中,亟需进行术中血流灌注实时监测,以防止术中血管受损;在眼底激光治疗术中,亟需进行术中血流灌注实时监测,以准确定位患者眼底的非血流灌注区或视网膜新生血管(RNV)区,避免传统方法(仅根据术前荧光素血管造影定位)可能导致的定位偏差。考虑到上述眼科手术中的血流成像需求,本实验通过简捷可靠的耦合结构集成了 OCTA 系统与手术显微镜,实现了活体兔眼眼科模拟手术中的高分辨眼底血流灌注成像监测,并定量分析了血流灌注随眼内压的时空动态演变过程。所得各时间段血流成像的定量分析结果中,兔眼视网膜的血流密度与眼内压数值呈显著负相关关系,这一现象与已有研究的小鼠视网膜血流密度随眼内压的变化情况相符^[41],从侧面证明了所提 iOCTA 系统在监测血流成像结果方面的正确性与可行性。此外,基于相位稳定的谱域 OCT 系统,能够以 120 kHz 的 A-line 采集速度获取轴向分辨率为 2.3 μm 、信噪比为 102 dB 的成像结果。横向对比已有 iOCTA 研究的相关技术指标(基于扫频 OCT 系统,A-line 采集速度为 100 kHz,轴向分辨率约为 5 μm 和 7.3 μm ,信噪比为 102 dB)^[34-35],所提 iOCTA 系统理论上能够以更快的成像速度实现高信

噪比成像,所获血流成像结果有更优的轴向分辨率和血流造影运动对比度。

尽管所提 iOCTA 系统已经实现了术中高分辨血流成像,但对于人眼的临床手术,iOCTA 系统还需要提升光能利用率和成像实时性,并消除成像伪影。对于光能利用率的提升,由于现有商用手术显微镜的最优成像波段为可见光波段(透过率在 95% 以上),在 OCT 成像波段[(850 \pm 50) nm]物镜的透过率约为 90%,有一定的光能损失,因此未来的研究将考虑改进显微物镜的镀膜技术,使显微物镜能够在可见光和 OCT 成像波段均有尽可能高的透过率。对于成像实时性的提升,可以使用线扫描速率更高的光谱仪线阵相机(例如线扫描速率为 250 kHz 的线阵相机),减少每个 A-line 数据的获取时间;或在更小的扫描范围下(例如对应兔眼视网膜范围为 2 mm \times 2 mm),适当减少扫描数据在 X、Y 方向的像素值,可以在不影响横向像素分辨率的前提下提升成像速度。对于不同种类成像伪影的消除,可以利用固定术中眼球的方法或者利用眼动追踪系统和运动矫正技术来消除眼球运动产生的运动伪影,通过重建算法来消除由表层血管的多重散射效应导致的较深视网膜层中的投影伪影^[6,42-43]。在未来的研究中,将结合上述各方面考虑和后续工作中的手术需求,进一步优化术中血流成像质量。

此外,眼科模拟手术仍存在进一步发展的空间。实际眼科手术中眼内压会因为不同的手术种类和术中操作存在不同程度的波动,包括眼内压峰值的不同或眼内压波动的持续时间不同^[44],未来的研究将考虑进一步根据玻璃体切除术等手术常见持续时间来增补更多灌注时间的实验组(分为长时、短时组),或者可进一步根据术中常见眼内压波动来增补更低或更高灌注压的实验组(分为轻度、中度、重度眼内压波动组),以更全面地模拟实际眼科手术的过程。进一步地,可考虑将 iOCTA 系统应用到临床试验中,在实际的白内障超声乳化手术、玻璃体切除术或眼底激光治疗术中进行眼底血流实时监测,深入研究术中实际操作、术后相关并发症与术中眼底血流成像的关联机制。

5 结论

提出一种集成手术显微镜的术中光学相干断层扫描血管造影(iOCTA)系统来实现高分辨的术中结构和血流造影成像。利用该 iOCTA 系统实现了活体兔眼眼科模拟手术中的眼底血流灌注成像,并通过定量的纵向分析揭示了血流灌注随眼内压的时空动态演变过程。所获结果表明,该 iOCTA 系统能够实现术中眼底血流状态的高分辨监测,有助于外科医生客观评价手术过程和预测术后效果,可广泛应用于眼科临床手术。

参 考 文 献

- [1] Findl O, Strenn K, Wolzt M, et al. Effects of changes in

- intraocular pressure on human ocular haemodynamics [J]. *Current Eye Research*, 1997, 16(10): 1024-1029.
- [2] Perente I, Utine C A, Ozturker C, et al. Evaluation of macular changes after uncomplicated phacoemulsification surgery by optical coherence tomography[J]. *Current Eye Research*, 2007, 32(3): 241-247.
- [3] Augustin M, Fialová S, Fischak C, et al. Ocular fundus pulsations within the posterior rat eye: chorioscleral motion and response to elevated intraocular pressure[J]. *Scientific Reports*, 2017, 7: 8780.
- [4] Chu Z D, Chen C L, Zhang Q Q, et al. Complex signal-based optical coherence tomography angiography enables *in vivo* visualization of choriocapillaris in human choroid[J]. *Journal of Biomedical Optics*, 2017, 22: 121705.
- [5] Moulton E M, Waheed N K, Novais E A, et al. Swept-source optical coherence tomography angiography reveals choriocapillaris alterations in eyes with nascent geographic atrophy and drusen-associated geographic atrophy[J]. *Retina*, 2016, 36(S1): S2-S11.
- [6] Chen C L, Wang R K. Optical coherence tomography based angiography[J]. *Biomedical Optics Express*, 2017, 8(2): 1056-1082.
- [7] Li P, Huang Z Y, Yang S S, et al. Adaptive classifier allows enhanced flow contrast in OCT angiography using a histogram-based motion threshold and 3D Hessian analysis-based shape filtering[J]. *Optics Letters*, 2017, 42(23): 4816-4819.
- [8] Li P, Cheng Y X, Li P, et al. Hybrid averaging offers high-flow contrast by cost apportionment among imaging time, axial, and lateral resolution in optical coherence tomography angiography [J]. *Optics Letters*, 2016, 41(17): 3944-3947.
- [9] Li P, Cheng Y X, Zhou L P, et al. Single-shot angular compounded optical coherence tomography angiography by splitting full-space B-scan modulation spectrum for flow contrast enhancement[J]. *Optics Letters*, 2016, 41(5): 1058-1061.
- [10] Guo L, Li P, Pan C, et al. Improved motion contrast and processing efficiency in OCT angiography using complex-correlation algorithm [J]. *Journal of Optics*, 2016, 18(2): 025301.
- [11] 李培, 李鹏. 多样本光学相干血流运动造影技术及应用[J]. *中国激光*, 2018, 45(3): 0307001.
Li P, Li P. Mass sample optical coherence tomography angiography technology and application[J]. *Chinese Journal of Lasers*, 2018, 45(3): 0307001.
- [12] 李培, 杨姗姗, 丁志华, 等. 傅里叶域光学相干层析成像技术的研究进展[J]. *中国激光*, 2018, 45(2): 0207011.
Li P, Yang S S, Ding Z H, et al. Research progress in Fourier domain optical coherence tomography [J]. *Chinese Journal of Lasers*, 2018, 45(2): 0207011.
- [13] Posarelli C, Sartini F, Casini G, et al. What is the impact of intraoperative microscope-integrated OCT in ophthalmic surgery? Relevant applications and outcomes. A systematic review[J]. *Journal of Clinical Medicine*, 2020, 9(6): 1682.
- [14] Spaide R F, Klancnik J M, Jr, Cooney M J. Retinal vascular layers imaged by fluorescein angiography and optical coherence tomography angiography[J]. *JAMA Ophthalmology*, 2015, 133(1): 45-50.
- [15] Liu K Y, Zhu T P, Yao L, et al. Noninvasive OCT angiography-based blood attenuation measurements correlate with blood glucose level in the mouse retina [J]. *Biomedical Optics Express*, 2021, 12(8): 4680-4688.
- [16] Yang S S, Liu K Z, Ding H J, et al. Longitudinal *in vivo* intrinsic optical imaging of cortical blood perfusion and tissue damage in focal photothrombosis stroke model[J]. *Journal of Cerebral Blood Flow and Metabolism*, 2019, 39(7): 1381-1393.
- [17] 刘颖, 杨亚良, 岳献. 光学相干层析血管造影术及其在眼科学中的应用[J]. *激光与光电子学进展*, 2020, 57(18): 180002.
Liu Y, Yang Y L, Yue X. Optical coherence tomography angiography and its applications in ophthalmology[J]. *Laser & Optoelectronics Progress*, 2020, 57(18): 180002.
- [18] 刘玉滨, 陈智毅, 袁振. 光学相干断层成像术评估细菌诱导性炎症[J]. *中国激光*, 2020, 47(2): 0207034.
Liu Y B, Chen Z Y, Yuan Z. Assessment of bacterial inflammation based on optical coherence tomography angiography [J]. *Chinese Journal of Lasers*, 2020, 47(2): 0207034.
- [19] 杨珊珊, 姚霖, 刘开元, 等. 光学相干层析功能成像及脑中风研究进展[J]. *中国激光*, 2020, 47(2): 0207015.
Yang S S, Yao L, Liu K Y, et al. Advances in functional optical coherence tomography and neuroimaging of stroke[J]. *Chinese Journal of Lasers*, 2020, 47(2): 0207015.
- [20] 史国华, 丁志华, 戴云, 等. 光纤型光学相干层析技术系统的眼科成像[J]. *中国激光*, 2008, 35(9): 1429-1431.
Shi G H, Ding Z H, Dai Y, et al. Ophthalmic imaging by optical coherence tomography [J]. *Chinese Journal of Lasers*, 2008, 35(9): 1429-1431.
- [21] Ehlers J P. Intraoperative optical coherence tomography: past, present, and future[J]. *Eye*, 2016, 30(2): 193-201.
- [22] Ehlers J P, Goshe J, Dupps W J, et al. Determination of feasibility and utility of microscope-integrated optical coherence tomography during ophthalmic surgery: the DISCOVER study RESCAN results[J]. *JAMA Ophthalmology*, 2015, 133(10): 1124-1132.
- [23] Pfaff M, Michels S, Binder S, et al. Clinical experience with the first commercially available intraoperative optical coherence tomography system[J]. *Ophthalmic Surgery, Lasers and Imaging Retina*, 2015, 46(10): 1001-1008.
- [24] Carrasco-Zevallos O M, Keller B, Viehland C, et al. Live volumetric (4D) visualization and guidance of *in vivo* human ophthalmic surgery with intraoperative optical coherence tomography[J]. *Scientific Reports*, 2016, 6: 31689.
- [25] Keller B, Draelos M, Tang G, et al. Real-time corneal segmentation and 3D needle tracking in intrasurgical OCT [J]. *Biomedical Optics Express*, 2018, 9(6): 2716-2732.
- [26] Tao Y K, Srivastava S K, Ehlers J P. Microscope-integrated intraoperative OCT with electrically tunable focus and heads-up display for imaging of ophthalmic surgical maneuvers [J]. *Biomedical Optics Express*, 2014, 5(6): 1877-1885.
- [27] Price F W, Jr. Intraoperative optical coherence tomography: game-changing technology[J]. *Cornea*, 2021, 40(6): 675-678.
- [28] Au J, Goshe J, Dupps W J Jr, et al. Intraoperative optical coherence tomography for enhanced depth visualization in deep anterior lamellar keratoplasty from the PIONEER study [J]. *Cornea*, 2015, 34(9): 1039-1043.
- [29] Hahn P, Migacz J, O'Donnell R, et al. Preclinical evaluation and intraoperative human retinal imaging with a high-resolution microscope-integrated spectral domain optical coherence tomography device[J]. *Retina*, 2013, 33(7): 1328-1337.
- [30] Ehlers J P, Dupps W J, Kaiser P K, et al. The prospective intraoperative and perioperative ophthalmic ImagiNg with optical CoherEncE TomogRaphy (PIONEER) study: 2-year results [J]. *American Journal of Ophthalmology*, 2014, 158(5): 999-1007.
- [31] Schechet S A, Komati R, Blair M P. Update on intraoperative OCT for vitreoretinal surgery: a new technology impacting surgical technique, management, and decision-making [J]. *Retinal Physician*, 2020, 17(1): 34-36.
- [32] Pasricha N D, Shieh C, Carrasco-Zevallos O M, et al. Needle depth and big-bubble success in deep anterior lamellar keratoplasty: an *ex vivo* microscope-integrated OCT study[J]. *Cornea*, 2016, 35(11): 1471-1477.
- [33] Steven P, le Blanc C, Lankenau E, et al. Optimising deep anterior lamellar keratoplasty (DALK) using intraoperative online optical coherence tomography (iOCT) [J]. *The British Journal of Ophthalmology*, 2014, 98(7): 900-904.
- [34] Chen X, Viehland C, Carrasco-Zevallos O M, et al. Microscope-integrated optical coherence tomography angiography in the

- operating room in young children with retinal vascular disease [J]. *JAMA Ophthalmology*, 2017, 135(5): 483-486.
- [35] Zhang Z Y, Zhu T P, Cao T T, et al. Swept source intraoperative OCT angiography [J]. *Journal of Innovative Optical Health Sciences*, 2021, 14(1): 2140009.
- [36] Huang L Z, Fu Y M, Chen R X, et al. SNR-adaptive OCT angiography enabled by statistical characterization of intensity and decorrelation with multi-variate time series model [J]. *IEEE Transactions on Medical Imaging*, 2019, 38(11): 2695-2704.
- [37] Chen R X, Yao L, Liu K Y, et al. Improvement of decorrelation-based OCT angiography by an adaptive spatial-temporal kernel in monitoring stimulus-evoked hemodynamic responses [J]. *IEEE Transactions on Medical Imaging*, 2020, 39(12): 4286-4296.
- [38] Li H K, Liu K Y, Yao L, et al. ID-OCTA: OCT angiography based on inverse SNR and decorrelation features [J]. *Journal of Innovative Optical Health Sciences*, 2021, 14(1): 2130001.
- [39] Li H K, Liu K Y, Cao T T, et al. High performance OCTA enabled by combining features of shape, intensity, and complex decorrelation [J]. *Optics Letters*, 2021, 46(2): 368-371.
- [40] Zhang Y M, Li H K, Cao T T, et al. Automatic 3D adaptive vessel segmentation based on linear relationship between intensity and complex-decorrelation in optical coherence tomography angiography [J]. *Quantitative Imaging in Medicine and Surgery*, 2021, 11(3): 895-906.
- [41] Zhi Z W, Cepurna W, Johnson E, et al. Evaluation of the effect of elevated intraocular pressure and reduced ocular perfusion pressure on retinal capillary bed filling and total retinal blood flow in rats by OMAG/OCT [J]. *Microvascular Research*, 2015, 101: 86-95.
- [42] Kraus M F, Potsaid B, Mayer M A, et al. Motion correction in optical coherence tomography volumes on a per a-scan basis using orthogonal scan patterns [J]. *Biomedical Optics Express*, 2012, 3(6): 1182-1199.
- [43] Zhang M, Hwang T S, Campbell J P, et al. Projection-resolved optical coherence tomographic angiography [J]. *Biomedical Optics Express*, 2016, 7(3): 816-828.
- [44] Moorhead L C, Gardner T W, Lambert H M, et al. Dynamic intraocular pressure measurements during vitrectomy [J]. *Archives of Ophthalmology*, 2005, 123(11): 1514-1523.

Intraoperative Optical Coherence Tomography Angiography with Micro Integration

Zhang Ziyi¹, Yu Chenyang¹, Qiao Yilin³, Shen Lijun³, Cheng Dan³, Li Peng^{1,2*}

¹ College of Optical Science and Engineering, Zhejiang University, Hangzhou 310027, Zhejiang, China;

² Intelligent Optics & Photonics Research Center, Jiaxing Research Institute, Zhejiang University, Jiaxing 324000, Zhejiang, China;

³ Fundus Center, Eye Hospital of Wenzhou Medical University at Hangzhou, Hangzhou 310020, Zhejiang, China

Abstract

Objective Acute ocular hypertension during ophthalmic surgery may lead to decreased retinal blood perfusion, nerve cell damage, and serious postoperative complications. Thus, in depth intraoperative blood perception is required, which standard surgical microscopes supply limitedly. Fluorescein angiography (FA), a traditional method for evaluating retinal blood flow, necessitates injecting fluorescent markers into the subject, which can be time consuming, invasive, and cause various side effects. Optical coherence tomography angiography (OCTA), as a functional extension of optical coherence tomography (OCT), provides a noninvasive, capillary level, and unmarked three-dimensional (3D) blood perfusion using flowing red blood cells (RBCs) as intrinsic agents. Recent developments in high-speed OCT systems and efficient OCTA algorithms promote the clinical practice of OCTA. Here, several microscope-integrated OCT/OCTA systems have been reported, which suggest that iOCT can improve the quality of posterior and anterior segment surgery. However, directly applying the current design to the commercial surgical microscope is difficult because of the interference with surgical ergonomics, and few studies are available intraoperative angiography because of the low contrast between capillaries and retinal tissue in OCT.

Methods A microscope-integrated intraoperative OCTA (iOCTA) system, based on a commercial surgical microscope (OPMI Lumera 300, Carl Zeiss, Germany), is developed for structural and angiographic imaging. The iOCTA system uses an SLD and a high-speed spectrometer, offering the central wavelength of 850 nm, a full width at half maximum bandwidth of 200 nm, A-scan rate of 120 kHz, range of imaging depth of ~ 2.6 mm, and axial resolution of ~ 2.3 μm in air. A simple and reliable adapter is designed to couple the imaging lightpath of the microscope and the OCTA through the assistant microscope port from the side, allowing the OCT and microscope to focus simultaneously. This coupling method maintains the surgical ergonomics design of the surgical microscope and can conveniently upgrade the commercial surgical microscope. A noncontact wide angle observation system is used to achieve fundus imaging. A charge-coupled device (CCD) camera is linked to the surgical microscope to capture images or record videos. The feasibility of the proposed iOCTA system is confirmed by monitoring the blood perfusion of a live rabbit's eyes during ophthalmic surgery. Acute ocular hypertension during cataract surgery or vitrectomy is simulated by artificially changing the intraocular pressure (IOP) of the rabbit's eyes. The main stages of the ophthalmic surgery included puncturing the sclera, maintaining IOP at

60 mmHg for 10 min, and recovering IOP to the normal value for 1 h. A series of representative intraoperative angiography of the rabbit's eyes is obtained in different stages during surgery. With 400 A-scans per B-scan, three repeated B-scans (in the X-direction) per lateral location, and 400 lateral locations (in the Y-direction) per 3D data, an OCTA scan is completed in ~ 4.8 s. To accurately distinguish dynamic blood flow regions and static surrounding tissues, the inverse signal-to-noise ratio (iSNR)-decorrelation OCTA (ID-OCTA) algorithm is used, where a classification line is set in a 1D space along the 3σ boundary of the distribution of static signals to remove the static tissues. By reconstruction and projection, a two-dimensional en-face image of OCTA containing dynamic signals of the whole 3D data is further achieved. Moreover, quantitative analysis of vessel density is performed to demonstrate longitudinal *in-vivo* optical imaging of retinal blood during surgery.

Results and Discussions Compared with the image captured by the CCD camera of the surgical microscope, high-resolution iOCTA obtained by the iOCTA system not only visualizes more capillary details but also improves the contrast of imaging at the capillary level (Fig. 2). The en-face images of OCTA in Fig. 3 reveal that retinal capillary filling is extinguished, and the diameter of the big vessels reduce within the peak IOP (60 mmHg). Capillary filling and the diameter of the big vessels recover within 3 min after the intraocular pressure acutely decreases to the initial value. The vessel density trend in Fig. 4 reveals that the retinal vessel density decreases significantly (reduced to below 20% of the baseline) within 1 min when the IOP increases acutely during surgery, decreases mildly within 10 min of maintaining peak IOP (60 mmHg), and rapidly rises to the initial vessel density within 2 min when the IOP returns to normal. En-face images of OCTA and the trend of vessel density demonstrate the negative correlation between blood perfusion and the value of IOP.

Conclusions This work presents an iOCTA system based on a commercial surgical microscope, which provides the dynamic monitoring of intraoperative retinal blood perfusion. High-resolution intraoperative blood perfusion imaging of a live rabbit's eyes is acquired using this iOCTA system during ophthalmic surgery. A series of representative en-face images of iOCTA and the trend of vessel density reveal the spatiotemporal dynamic evolution of blood perfusion. Real-time monitoring of retinal blood perfusion during ophthalmic surgery is expected to be realized using this iOCTA system, which will help surgeons objectively evaluate the surgical procedures and predict postoperative effects.

Key words medical optics; medical and biological imaging; optical coherence tomography; optical coherence tomography angiography; intraoperative imaging